CaS: Sb^{3+}, Na and ZnS:Sn^{2+}: phosphor materials for the improvement of WLEDs

Phuc Dang Huu[1], Ton That Phung[2]

[1]Institute of Applied Technology, Thu Dau Mot University, Binh Duong Province, Vietnam
[2]Faculty of Electronics Technology, Industrial University of Ho Chi Minh City, Ho Chi Minh City, Vietnam

Article Info	ABSTRACT
	The remote phosphor configuration, though not the best choice for white light-emitting diodes (WLED) color quality, is superior to the luminous flux of LEDs compared to the conformal or in-cup structures. Realizing the capability of the remote phosphor design, several studies have been done to overcome the drawback of this structure, and which is the color quality. A two-film distant phosphor configuration with improved color rendering index (CRI) and color quality ratio (CQS) for WLEDs is offered in this study paper. The hue temperature of the WLEDs packets employed in this research is 8500 K. This phosphor structure is constructed by layering of a green CaS: Sb^{3+}, Na or red ZnS: Sn^{2+} phosphor above the yellow YAG: Ce^{3+} phosphor. The additional phosphor ZnS: Sn^{2+} concentration will then be modified to get the best color quality. The results demonstrated an increase in CRI and CQS along with the presence of ZnS: Sn^{2+}, indicating that the existence of ZnS: Sn^{2+} influences significantly on these two aspects. As a result of the increased concentration of red illumination elements inside packets, the higher the concentration of ZnS: Sn^{2+}, the higher the CRI and CQS. The green phosphor CaS: Sb^{3+}, Na, in the meantime, improves the luminous flux. *This is an open access article under the CC BY-SA license.*

Corresponding Author:

Ton That Phung
Faculty of Electronics Technology, Industrial University of Ho Chi Minh City
No. 12 Nguyen Van Bao Street, Ho Chi Minh City, Vietnam
Email: tonthatphung@iuh.edu.vn

1. INTRODUCTION

White light-emitting diodes (WLEDs) have piqued the interest of researchers because of their outstanding advantages to conventional illumination sources, such as excellent performance, reduced consumption, environmental safety, and longer lifespan [1], [2]. The most popular type of WLED is the phosphor-transformed WLED (pc-WLED), which combines a blue LED chip with the phosphor emits the yellow color $Y_3Al_5O_{12}$:Ce^{3+} (YAG: Ce^{3+}). Despite having a high lighting efficiency (LE), pc-WLEDs have a low CRI (70) owing to the absence of red spectral components [3]-[5]. The utilization of red phosphor is an effective method for repairing the CRI issue. However, because the wide red emission is mainly located beyond the sensitive area of human vision, maintaining high LE is impossible [6]-[8]. Quantum dots (QDs) have lately sparked a lot of attention in the solid-state lighting sector due to their unique optical properties such as limited radiation spectrum, size-adjustable radiation wavelength, and great quantum outputs [9], [10]. WLEDs made up of a blue LEDchip, a yellow-emitting phosphor, and a red-emitting QD have been reported to have an excellent CRI (Ra>90) and an extremely high LE, making them a potential option for the upcoming artificial source of illumination. QDs are inappropriate for immediate integration of LEDs in QDs-WLEDs packaging techniques due to their solution-based combination technique, in which QDs are

immersed in some organic solvent. The hydrophobic organic ligands on the outside of QDs have a deleterious influence on silicone gel polymerization, especially the catalyst-poisoning influence. Furthermore, the mismatch of the outside of QDs with silicone gel might lead to QD aggregation, lowering the photolumi-nescence (PL) efficiency [11]-[13]. As a response, many solutions to the compatibility problem have been offered, such as changing the surface chemistry of QDs, integrating QDs into mesoporous microspheres, or putting a barrier layer on the surface of QDs. QDs-silica covered nanoparticles (QSNs), such as CdSe-SiO₂, CdSe/ZnS-SiO₂, and CdSe/CdS/ZnS-SiO₂, have received a lot of attention, and the QSNs/phosphor silicone combination photostability has been demonstrated to be substantially enhanced after covering in comparison with other methods [14]-[16]. Current QSNs-WLEDs, according to our understanding, are created by immediately mixing QSNs with phosphor gel. Owing to the significant Mie-scattering impact of phosphor particles, yellow photons are partly re-imbibed by QSNs and changed to red photons, resulting in reabsorption power losses. Additionally, applying QSNs is considered ineffective since the space among the nanosized QSNs and the LED chip is significant, increasing the required QDs amount [17], [18]. Hence, the QDs surfaces in this study were covered by a siliva shell to overcome the compatibility issue among QDs and phosphor-silicone gel. Next, to reduce reabsorption power loss, a QSNs-on-chip packing configuration was developed. The suggested QSNs-on-chip packaging and traditional combined packing are depicted schematically in Figure 1. A microemulsion reaction was used to create QSNs from red-emitting CdSe/ZnS core–shell QDs. QSNs were covered straight onto the LED chip for the manufacture of QSNs-on-chip WLEDs packing, and then a yellow-emitting YAG: Ce^{3+} phosphor silicone gel was applied. This study also addressed the influence of QD/phosphor reabsorption on optical power loss. Finally, in order to investigate the thermal effect caused by reabsorption energy loss, the temperature ranges of the QSNs-on-chip as well as traditional mixed QSNs-WLEDs were brought into evaluation.

2. DETAIL OF EXPERIMENT AND SIMULATION

2.1. Preparation of phosphor materials

$ZnS: Sn^{2+}$ is one of the two main phosphors applied in this study. This phosphor has a hexagonal (wurtzite) configuration, a red emission color, and an emission peak at 1.80 eV. Additionally, its emission width (FWHM) is 0.40 eV and stimulation efficiencies by UV are at +(4.88 eV) and ++(3.40 eV). The composition to modulate this phosphor is detailed in the Table 1. The first step to modulate $ZnS: Sn^{2+}$ is to combine the ingredients by grinding it all together. Then, the mixture needs to be heated up in capped quartz tube with N_2 at 1150°C for 1 hour [19], [20].

The name of the other phosphor used in this study is CaS: Sb^{3+}, Na. With a cubic (NaCl) structure, its optical properties include yellow-green radiation color, radiation reach the maximum point at 2.27 eV and emission width (FWHM) is 0.44 eV. Furthermore, the excitation efficiency of this phosphor are at ++(4.88 eV) and –(3.40 eV) by UV and 18% by e-beam. Lastly, CaS: Sb^{3+}, Na decays exponentially (~1.5 µsec to 1/10), following by a long but faint tail of phosphorescence. The composition to modulate it is listed in the Table 2.

Table 1. Composition of $ZnS: Sn^{2+}$			Table 2. Composition of CaS: Sb^{3+}, Na		
Ingredient	Mole %	By weight (g)	Ingredient	Mole %	By weight (g)
ZnS	99	97	CaCO₃	100	100
SnS	1	1.5	Sb₂CO₃	0.1 (of Sb)	0.145
Sulfur		~2-3	NaHCO₃	1	0.840

There are two options of preparation CaS:Sb^{3+},Na. The first way is to heat CaCO₃ (the purest) in open quartz boats with H_2S for 1 hour at 1100°C and then make it into powder. Next, adding in the amount that mentioned before of Sb₂O₃+NaHCO₃ along with ~ 2-3 g of sulfur and combine those all together by dry grinding. The second option is to firstly fire the ingredients in covered alumina crucibles with N_2 at 1300°C for 1 hour and also make them into powder. Last but not least, this requires preservation in a well-closed container [21], [22].

2.2. Stimulation process

There are two dual-film phosphor configuration models recommended in this paper, which are the green-yellow configuration (GYC) and the red-yellow configuration (RYC). Those two configurations are built using two phosphor coatings on blue chips. In particular, in the GYC configuration, as illustrated in Figure 1(a), the phosphor CaS: Sb^{3+}, Na layer lies on top the YAG: Ce^{3+} yellow phosphor film. In the meantime, in the RYC one, the phosphor layer placed above the YAG: Ce^{3+}+ layer is $ZnS: Sn^{2+}$, as shown in Figure 1(b). Increase the WLEDs color quality and lumen efficacy is the aim of utilizing GYC and RYC. This may be accomplished by inserting into the WLED packages the green dispersing and red illumination

components. Yet, the CaS: Sb^{3+}, Na and ZnS: Sn^{2+} concentration must be altered correspondingly to be able to perform this.
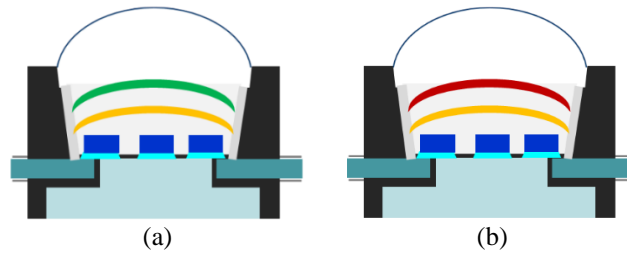

Figure 1. two models dual-film phosphor configuration (a) picture of GYC and (b) picture of RYC

As shown in Figure 2(a) and Figure 2(b), the concentrations of red and green phosphors vary in the adverse direction to those of yellow phosphor. This distinct adjustment will preserve average CCTs while influencing the dispersing and absorptivity of WLEDs phosphor films. This will clearly have a significant impact on the color quality and the illuminating beam of the LED lights as well. As a result, choosing the concentration of CaS: Sb^{3+}, Na and ZnS: Sn^{2+} is a vital factor in increasing the hue standard of the WLED. Particularly, even with a high hue temperature of 8500 K, the YAG: Ce^{3+} concentration still declines to preserve the average CCT when the CaS: Sb^{3+}, Na and ZnS: Sn^{2+} concentrations raise 18% (2%-26% wt).
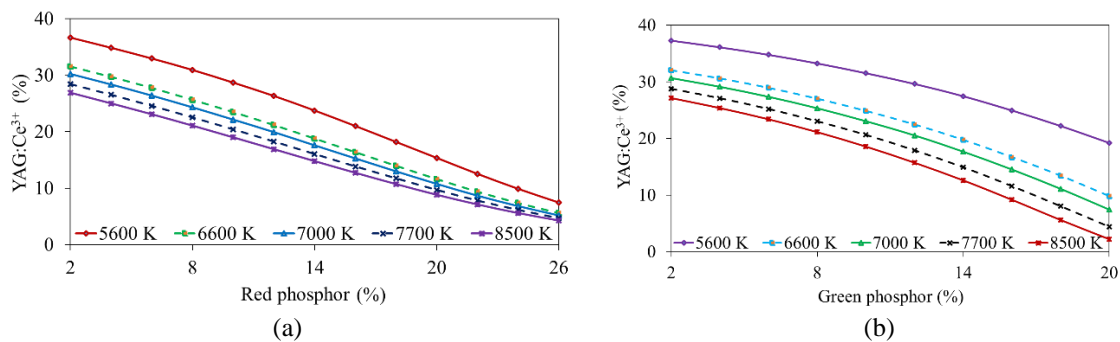

Figure 2. The phosphor concentrations of (a) RYC and (b) GYC were shifted to maintain the mean CCT

Furthermore, as seen in Figure 3, red ZnS: Sn^{2+} concentrations have a considerable influence on the spectrum of WLEDs. The red-yellow structure appears to enhance in spectrum emission in three separate areas when compared to the green phosphor CaS: Sb^{3+}, Na configuration. When the concentration of CaS: Sb^{3+}, Na develops, the intensity in the spectral ranges from 420 nm to 480 nm and 500 nm to 640 nm rises, as shown in Figure 3(a). Speaking differently, a greater in luminous flux is indicated by a rise in the emission spectra in two of these locations. Furthermore, using CaS: Sb^{3+}, Na creates more internal blue-light scattering activities, which suggests an increase in phosphor dispersing inside the LEDs, benefiting the copper color. In the mean time, when the concentration of ZnS: Sn^{2+} increases, so does the radiation spectra in the region of 648 nm to 738 nm. However, owing to the absence of the increased radiation spectra in the two comparable areas of 420 nm-480 nm and 500 nm-640 nm, this improvement is unnecessary, since enhancing the strength of these two spectral areas will benefit the luminous flux of the light of blue (blue-light dispersing). Another impact shown in Figure 3(b) is an augmentation in emission spectra associated with a rise in color temperature. Put it in another way, the greater the color temperature, the stronger the spectral radiation. As a result, improved color and optical performance is conceivable. This finding is critical for LED manufacturers who use the ZnS: Sn^{2+} phosphor, specifically when managing the elevated temperature WLEDs' quality is difficult. In summary, the fact that red phosphor ZnS: Sn^{2+} is able to improve the hue performance of WLEDs with high color temperatures (8500 K) is analyzed in this research. The structure can be chosen according to the manufacturers' specifications. A modest drop in luminous flux is acceptable if they decide to make WLEDs with great color quality.
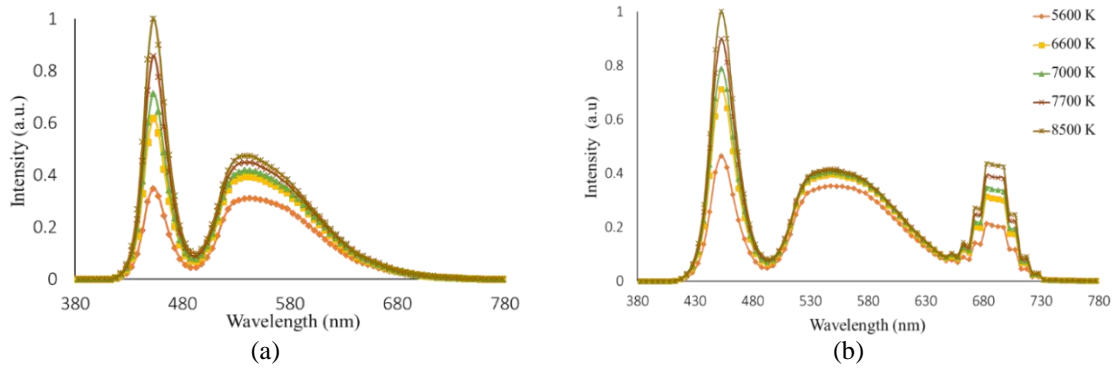
Figure 3. Radiation spectra of (a) RYC and (b) GYC

3. COMPUTATION AND DISCUSSION

The CRI is a mensuration which is applied to assess how well an illumination origin displays the real hue of things when compared to natural light, see Figure 4(a). According to the color theory of the three main hues, which are red, yellow, and green, the hue disparity arises when the green illumination element is greater than the rest. Therefore, the WLEDs hue quality suffers and decreasing their color fidelity. The graphs in Figure 4(b) show the drop in CRI when adding the green phosphor $CaS:Sb^{3+}$,Na. Particularly, the CRI drops progressively when this phosphor's concentration rises from 2% to 20%. When compared to CQS, CRI is not an optimum measure since it can not assess all features of light quality. As a result, the CRI drops caused by $CaS:Sb^{3+}$,Na are tolerable. Regarding to CQS, it is a synthesis of three essential parts: CRI, human preferences, and hue coordinates. As a consequence, CQS is a more critical objective that is more difficult to attain. CQS keeps its high values when the $CaS:Sb^{3+}$,Na concentration does not exceed 8%, based on the data presented in Figure 5(a). On the contrary, the CQS reduces considerably as the $CaS:Sb^{3+}$,Na concentration increases from 8% to 26%, see Figure 5(b). As a result, after accounting for the emitted luminous flux, if the objective is to enhance hue standard, an adequately chosen concentration of $CaS: Sb^{3+}$, Na can range from 2% to 8%.

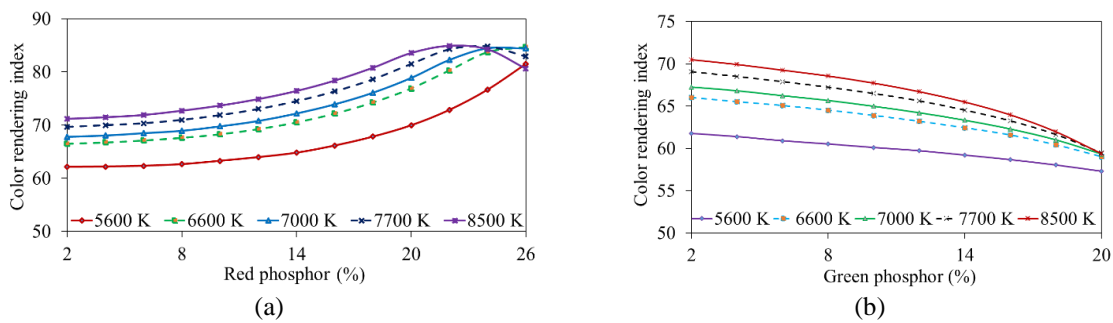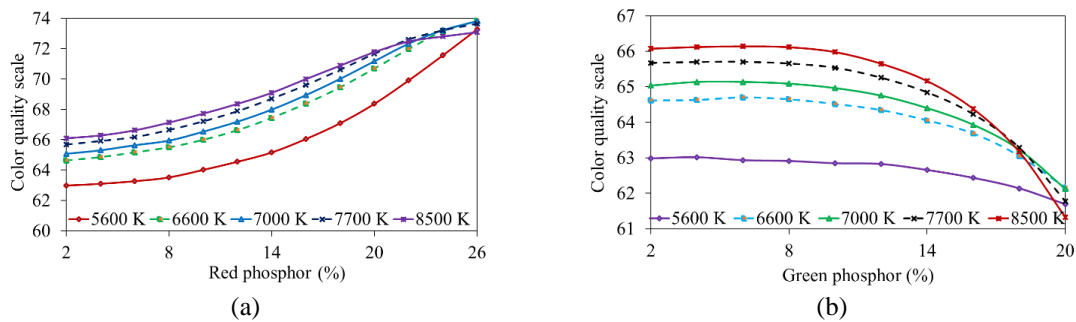Figure 4. The hue rendering indicator as a function of the concentration of $CaS:Sb^{3+}$,Na, and $ZnS:Sn^{2+}$ (a) RYC and (b) GYC

Figure 5. The hue quality ratio as a function of the concentration of $CaS: Sb^{3+}$, Na and $ZnS: Sn^{2+}$ (a) RYC and (b) GYC

As with the CRI, Figure 5 reveals that the red phosphor ZnS: Sn^{2+} can increase CQS levels. Figure 5's first graph shows that a considerable improvement in CQS corresponds to an increase in ZnS: Sn^{2+} concentration. Clearly, ZnS: Sn^{2+} concentration reachs the highest point (20%) while CQS is also at the maximum point (around 72). In the mean time, CaS: Sb^{3+}, Na concentration has the lower CQS than ZnS: Sn^{2+}, just reachs 66 and only equals with the smallest number of ZnS: Sn^{2+} concentration. As a result, we can deduce that utilizing ZnS: Sn^{2+} possibly improves the white illimination standard for WLEDs that use the dual-film phosphor configuration. This is among the most important discoveries for manufacturers to acknowledge when striving to improve color quality. However, ZnS: Sn^{2+} in fact has a negative impact on the WLEDs lumen output and should not be overlooked. This section will describe and illustrate the scientific subject of transferred blue lighting and transformed yellow lighting in a double-film phosphor design. Furthermore, achieving a significant increase in LED performance is feasible. Transferred blue lighting and transformed yellow lighting for a one-film distant phosphor module with *2h* phosphor film thickness is stated as shown in [23], [24]:

$$PB_1 = PB_0 \times e^{-2\alpha_{B1}h} \tag{1}$$

$$PY_1 = \frac{1}{2}\frac{\beta_1 \times PB_0}{\alpha_{B1} - \alpha_{Y1}}(e^{-2\alpha_{Y1}h} - e^{-2\alpha_{B1}h}) \tag{2}$$

For a dual-film distant phosphor arrangement with *h* phosphor film thickness, the transferred blue lighting and transformed yellow lighting are described as:

$$PB_2 = PB_0 \times e^{-2\alpha_{B2}h} \tag{3}$$

$$PY_2 = \frac{1}{2}\frac{\beta_2 \times PB_0}{\alpha_{B2} - \alpha_{Y2}}(e^{-2\alpha_{Y2}h} - e^{-2\alpha_{B2}h}) \tag{4}$$

Where *h* denotes the thickness of each film. The single-film and dual-film distant phosphor configuration are respectively represented by subscripts "1" and "2". The transformation factor for changing the light of blue to yellow is indicated as *β*, while *γ* represents the yellow lighting reflexion factor. Blue lighting *(PB)* and yellow lighting *(PY)* intensities are illumination intensities from blue LEDs, as denoted by PB_o. Furthermore, the percentages of power losing of blue and yellow photons in the phosphor layer independently during multiplication are characterized by two indices, *αB* and *αY*. The illumination efficiency of pc-LEDs is greater with a dual-layer phosphor arrangement than with a single layer configuration:

$$\frac{(PB_2 + PY_2) - (PB_1 + PY_1)}{PB_1 + PY_1} > 0 \tag{5}$$

The dispersing of phosphor particles was established using Mie-theory [25], and by using the following equation, the lighting cross section Csca for spherical particles may be calculated. Furthermore, the Lambert-Beer law could be applied to measure the transferred luminous energy:

$$I = I_0\, exp(-\mu_{ext}L) \tag{6}$$

Where I_o denotes the incident luminous energy, *L* is the phosphor film thickness (mm), and the extinction factor in this formula is indicated as *μext*. Furthermore, *μext* may be written as: *μext = Nr. Cext*. *Nr* is the particle density distribution (mm^{-3}) and C_{ext} (*mm^2*) expresses the extinction cross-section of phosphor particles.

The luminous efficiency of double-layer remote phosphor pc-LEDs appears to be higher than that of single-phosphor pc-LEDs, as demonstrated by expression (5). Consequently, the lumen effectiveness of the dual-film distant phosphor film utilized in LED packtes has been conducted and demonstrated in this research. In Figure 6(a), it can be seen that the illuminating beam increases as the CaS: Sb^{3+}, Na concentration increases 18% wt. (2% wt. - 20% wt.). On the contrary, the illuminating beam of the dual-layer remote phosphor structure gradually drops as the concentration of ZnS: Sn^{2+} phosphor increases. The Lambert-Beer equation obviously states that the decline factor *μext* is proportional to the ZnS: Sn^{2+} concentration and inversely proportional to the illumination transference power. As a result, the emitted photoluminescence may decrease as the ZnS: Sn^{2+} concentration increases if the two phosphors' thicknesses remain constant. The luminous flux produced by the the dual-film distant phosphor design (with a red phosphor film of ZnS: Sn^{2+}) is, however, greater than that produced by the single-film distant phosphor design (with no red phosphor film), as in expression (5). Furthermore, the CRI and CQS values benefit from this red phosphor. As a result of the benefits gained by employing ZnS: Sn^{2+}, the drop in lumen output is absolutely reasonable. Manufacturers can choose an appropriate ZnS: Sn^{2+} concentration for mass production of WLEDs relying on the goal they want to accomplish. Both varieties have high CRI ratings of Ra > 90 and R9 > 90 at the same corresponding color temperature level of 4700 K (neutral white light), indicating the color-rendering capacity toward deep red. As a result of the separated QSNs/phosphor construction,

the reabsorption energy loss between QSNs and phosphor can be minimized greatly. Both types of WLEDs exhibit stable spectral distributions without PL saturation, with CRI values remaining practically unaltered even at 200 mA (Ra > 88 and R9 > 89). Under varied driving currents, type I has higher LE than type II, and showing that reabsorption losses are effectively reduced. It should be noted that the decrease in LE with increasing current is primarily due to a decrease in the efficiency of the LED chip itself. To study the reabsorption effect further, we estimated the optical energy loss of an LED chip, QSNs plus phosphor in QSNs-on-chip type, and QSNs/phosphor combination in combined form. The optical energy difference during the packing process is used to calculate the energy losses. These reabsorption energy losses are also theoretically calculable, see Figure 6(b). In a nutshell, the energy loss of a "LED chip" is computed by subtracting the input electrical power from the output optical power of an LED module with only silicone gel; the distinction between the output optical optical power of an LED module with just silicone gel and the output optical optical power of an LED module with QSNs plus phosphor gel is used to determine the energy loss of "QSNs plus phosphor"; the difference between the output optical power of an LED module with just silicone gel and the output optical power of an LED module with mixed QSNs/phosphor gel is used to measure energy loss of "combination of QSNs/phosphor." Another major issue is that the operating temperature of QSNs-on-chip should be lower than that of combined form owing to decreased heat output. As a result, we used an infrared thermal imager to measure the constant temperature ranges of these two WLEDs. The WLEDs module is installed on a metal core printed circuit board for heat dissipation before being powered by 200 mA. The silicone gel's emissivity is set to 0.96, and the spacing between the camera lens and the WLEDs is set to 0.5 m. The temperature of top silicone in the QSNs-on-chip form is 20.5°C lower than that in the combined form under the same driving current of 200 mA. The peak temperature of QSNs-on-chip form is also located on the top surface of silicone, and it is lower than that of combined form due to QSNs' improved heat dissipation condition. Experiments prove that the QSNs-on-chip form outperforms the conventional combined form in both optical and thermal performance.
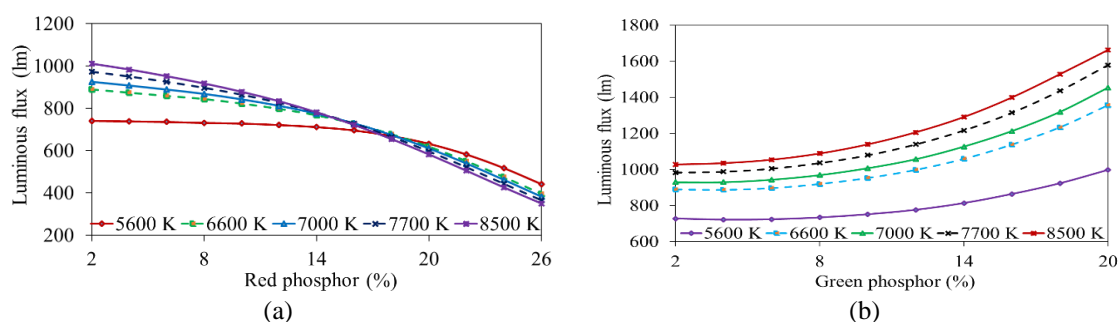

Figure 6. The lumen performance as a function of the concentration of CaS: Sb^{3+}, Na and ZnS: Sn^{2+} (a) RYC and (b) GYC

4. CONCLUSION

This paper illustrates the impact of green CaS: Sb^{3+}, Na, and red ZnS: Sn^{2+} phosphors on CRI, CQS, and illuminating beam of a dual-film phosphor structure. Using the Mie-scattering theory and the Lambert Beer's law, the researchers conclude that ZnS: Sn^{2+} is an appropriate phosphor substance for increasing hue standard, although CaS: Sb^{3+}, Na is still a good alternative for improving WLED illuminating beam. This is true not only for WLEDs with reduced hue temperatures, but also for those with significant hue temperatures of 8500 K. Finally, the goal of improving the white lighting hue standard that has been a difficult issue for distant-phosphor designs, has been accomplished. Nonetheless, there is one little disadvantage in regards to lighting beam: the color quality or luminous flux have the tendency to decline substantially when CaS: Sb^{3+}, Na or ZnS: Sn^{2+} concentrations are extremely high. Therefore, deciding a suitable concentration for the phosphors based on manufacturers' purposes is critical. Also, the research paper's findings may be utilized as a critical reference in the producing higher-quality WLED modules.

REFERENCES

[1]   S. Adachi, "Review—Mn^{4+}vs Cr^{3+}: A Comparative Study as Activator Ions in Red and Deep Red-Emitting Phosphors," *ECS Journal of Solid State Science and Technology*, vol. 9, no. 2, p. 026003, 2020.
[2]   H. Ming, J. Zhang, L. Liu, J. Peng, F. Du, and X. Ye, "Luminescent Properties of a Cs_3AlF_6:Mn^{4+} Red Phosphor for Warm White Light-Emitting Diodes," *ECS Journal of Solid State Science and Technology*, vol. 7, no. 9, p. R149, 2018.
[3]   H. Y. Jiao, C. R. LiMao, Q. Chen, P. Y. Wang, and R. C. Cai, "Enhancement of red emission intensity of $Ca_2Al_2SiO_7$:Eu^{3+} phosphor by MoO_3 doping or excess SiO_2 addition for application to white LEDs," *IOP Conference Series: Materials Science and Engineering*, vol. 292, no. 1, p. 012058, 2018.

[4]   Z. Yu, S. Man, P. He, N. Zhang, and C. Gu, "Preparation and Photo luminescent Properties of $Sr_2Si_5N_8$: Eu^{2+} Red Phosphors for White Light-Emitting Diodes," *IOP Conference Series: Earth and Environmental Science*, vol. 170, no. 4, p. 042114, 2018.

[5]   N. S. Zailani, M. F. Ghazli, R. Hussin, S. Z. Abd Rahim, and M. N. M. Saad, "Effects of Sm^{3+} on Luminescent Properties of $LiEu_{(0.55-x)}Y_{0.45}$ $(WO_4)_2Smx$ Red Phosphor," *IOP Conference Series: Materials Science and Engineering*, vol. 374, no. 1, pp. 012001, 2018.

[6]   L. T. Ha *et al.*, "Effect of doping concentration and sintering temperature on structure and photoluminescence properties of blue/red emitting bi-phase Eu^{3+}/Eu^{2+}-doped $Sr_5(PO_4)_3Cl/Sr_3(PO_4)_2$ phosphors," *Materials Research Express*, vol. 5, no. 7, p. 076516, 2018.

[7]   L. Yang, G. Jiang, D. Wu, and H. Chen, "Preparation of a Novel Red Y_2MoSiO_8: Eu^{3+}, Dy^{3+} Phosphor," IOP Conference Series: Earth and Environmental Science, vol. 714, no. 3, p. 032002, 2021.

[8]   J. Xie and X. Zhang, "Synthesis and photoluminescence properties of ultraviolet excited Ba^2MgWO_6:Sm^{3+} orange-red phosphors," IOP Conference Series: Earth and Environmental Science, vol. 639, no. 1, p. 012030, 2021.

[9]   S. Adachi, "Photoluminescence Spectroscopy and Crystal-Field Parameters of Cr^{3+} Ion in Red and Deep Red-Emitting Phosphors," *ECS Journal of Solid State Science and Technology*, vol. 8, no. 12, pp. R164, 2019.

[10] S. Cui and G. Chen, "Investigation of photoluminescence properties, quenching mechanism and thermal stability of the red-emitting phosphor based on Eu ions doped apatite host $NaLa_9(SiO_4)_6O_2$," Materials Research Express, vol. 6, no. 9, p. 096201, 2019.

[11] Y. Wang, Y. Wang, M. Wang, Y. Shao, and Y. Zhu, "Facile preparation and formation mechanism of $Sr_2Si_5N_8$:Eu^{2+} red-emitting phosphors," *Materials Research Express*, vol. 5, no. 5, p. 056202, 2018.

[12] X. Pan, D. Hou, M. Zhou, H. Lai, H. Ming, and X. Ye, "HF-Free Preparation, High Thermal and Color Stability of Mn^{4+} Activated K_2TiF_6 Red Phosphors for White Light-Emitting Diodes," *ECS Journal of Solid State Science and Technology*, vol. 7, no. 1, p. R3006, 2018.

[13] J. Silver, P. J. Marsh, G. R. Fern, T. G. Ireland, and A. Salimian, "ZnCdS:Cu,Al,Cl: A Near Infra-Red Emissive Family of Phosphors for Marking, Coding, and Identification," *ECS Journal of Solid State Science and Technology*, vol. 7, p. R3057. 2018.

[14] X. Ma, S. Sun, and J. Ma, "A novel orange-red $Sr_9Ga(PO_4)_7$: Sm^{3+} phosphors for white light emitting diodes," *Materials Research Express*, vol. 6, no. 11, pp. 116207, 2019.

[15] X. Zhang, R. Cui, J. Zhang, X. Qi, and C. Deng, "A Novel Red-Emitting Phosphor Ca_2GdNbO_6: Eu^{3+}: Influences of Sintering Temperature and Eu^{3+} Concentration on the Photoluminescence," *ECS Journal of Solid State Science and Technology*, vol. 10, no. 2, p. 026003, 2021.

[16] K. Su, Q. Zhang, X. Yang, and B. Ma, "Crystal structure and luminescence properties of thermally stable Sm^{3+}-doped $Sr_9In(PO_4)_7$ orange-red phosphor," *Journal of Physics D: Applied Physics*, vol. 53, no. 38, p. 385101, 2020.

[17] Y. V. Baklanova, L. G Maksimova, O. A. Lipina, A. P. Tyutyunnik, A. Y. Chufarov, and V. G. Zubkov, "A red-emitting phosphor based on Eu^{3+}-doped $Li_6SrLa_2Ta_2O_{12}$ garnets for solid state lighting applications," *Materials Research Express*, vol. 6, no. 6, p. 066201, 2019.

[18] G. Rahate, V. R. Panse, S. J. Dhoble, N. S. Kokode, and K. Sharma, "Photoluminescence studies and synthesis of $KSrPO_4$:Ce^{3+}, Eu^{3+} blue and orange-red emitting phosphor," *IOP Conference Series: Materials Science and Engineering*, vol. 1120, p. 012005, 2021.

[19] S. Adachi, "Review—Tanabe−Sugano Energy-Level Diagram and Racah Parameters in Mn^{4+}-Activated Red and Deep Red-Emitting Phosphors," *ECS Journal of Solid State Science and Technology*, vol. 8, no. 12, p. R183, 2019.

[20] L. Lei, Z. He, Z. Qun, Y. Chun-Feng, G. Chao-Chao, and L. Yi, "Influences of sol-gel progress on luminescent properties of $Li_{1.0}Nb_{0.6}Ti_{0.5}O_3$:$Eu^{3+}$ red phosphor," *Materials Research Express*, vol. 6, no. 6, p. 046202, 2019.

[21] C. He *et al.*, "Preparation and photoluminescence properties of red-emitting phosphor $ZnAl_2O_4$:Eu^{3+} with an intense $^5D_0 \rightarrow ^7F_2$ transition," *Materials Research Express*, vol. 5, no. 2, p. 025501, 2018.

[22] O. M. ten Kate, Y. Zhao, K. M. B. Jansen, J. R. van Ommen, and H. T. (Bert) Hintzen, "Effects of Surface Modification on Optical Properties and Thermal Stability of K_2SiF_6:Mn^{4+} Red Phosphors by Deposition of an Ultrathin Al_2O_3 Layer Using Gas-Phase Deposition in a Fluidized Bed Reactor," *ECS Journal of Solid State Science and Technology*, vol. 8, no. 6, p. R88, 2019.

[23] X. Yao, M. Cai, and S. Man, "Preparation and Properties of Cr^{3+} Doped $Mg_{0.388}Al_{2.408}O_4$ Red Phosphor," *IOP Conf. Ser.: Mater. Sci. Eng.*, vol. 782, no. 2, p. 022020, 2020.

[24] Q. Wei, Z. Yang, Z. Yang, Q. Zhou, and Z. Wang, "Communication—Luminescent Properties of Mn^{4+}-Activated K_3HfF_7 Red Phosphor," *ECS Journal of Solid State Science and Technology*, vol. 7, no. 5, p. R39, 2018.

[25] T. Pang and Z. Huang, "A novel upconverison phosphor $Gd_2Mo_4O_{15}$:Yb^{3+}, Ho^{3+}: intense red emission and ratiometric temperature sensing under 980 nm excitation," *Materials Research Express*, vol. 5, no. 6, p. 066204, 2018.

BIOGRAPHIES OF AUTHORS

Phuc Dang Huu received a Physics Ph.D degree from the University of Science, Ho Chi Minh City, in 2018. Currently, He is Research Institute of Applied Technology, Thu Dau Mot University, Binh Duong Province, Vietnam. His research interests include simulation LEDs material, renewable energy. He can be contacted at email: danghuuphuc@tdmu.edu.vn.

Phung Ton That was born in Thua Thien-Hue, Vietnam. He received the B.Sc. degree in electronics and telecommunications engineering (2007) and the M.Sc. degree in electronics engineering (2010) from the University of Technology, Vietnam. He is currently a lecturer at the Faculty of Electronics Technology (FET), Industrial University of Ho Chi Minh City. His research interests are optical materials, wireless communication in 5G, energy harvesting, performance of cognitive radio, physical layer security and NOMA. He can be contacted at email: tonthatphung@iuh.edu.vn